Variability of cool seasonal rainfall associated with Indo-Pacific climate modes: case study of Victoria, Australia

F. Mekanik and M. A. Imteaz

ABSTRACT

This study focused on diagnosing the relative and independent role of El Niño Southern Oscillation (ENSO) and Indian Ocean Dipole (IOD) on austral cool seasonal rainfall by stratifying the cool seasonal rainfall into winter (June–August) and spring (September–November). Partial regression and classification analysis was used to investigate the effect of the climate modes on rainfall in the state of Victoria in southeast Australia. Partial regression analyses revealed that when the influence of IOD is removed from ENSO, sea surface temperature (SST) anomalies in the Pacific Ocean have no significant effect on spring rainfall across Victoria and affect winter rainfall mildly in west Victoria. By removing the inter-correlations between ENSO and IOD, SST anomalies in the Indian Ocean and SLP anomalies in the Pacific Ocean showed weak relationships with Victoria's spring and winter rainfall. Classification analysis demonstrated the effects of phases of ENSO and IOD on Victoria's seasonal rainfall; the dry phases of the climate modes have more effect on spring rainfall compared to the wet phases and both show no significant effect on winter rainfalls. It is recommended that for water availability forecasting in Victoria, water managers should focus on the effect of climate modes on spring rainfalls, particularly during the dry phases of ENSO and IOD.

Key words | classification analysis, cool seasonal rainfall, ENSO, IOD, linear regression, partial regression

F. Mekanik (corresponding author)
M. A. Imteaz
Centre for Sustainable Infrastructure, School of Engineering,
Swinburne University of Technology,
Melbourne, VIC,
Australia
E-mail: *fmekanik@swin.edu.au*

INTRODUCTION

The El Niño Southern Oscillation (ENSO) and the Indian Ocean Dipole (IOD) affect the climate of many nations around the Pacific and Indian Ocean rim. Researchers have used different methods and modelling techniques in order to extract and model the relationships between the large-scale climate modes and rainfalls in different parts of the world (Lau & Weng 2001; Barsugli & Sardeshmukh 2002; Yufu *et al.* 2002; Hartmann *et al.* 2008; Chattopadhyay *et al.* 2010; Shukla *et al.* 2011; Ishak *et al.* 2013; Biabanaki *et al.* 2014; Hajani & Rahman 2017; Hajani *et al.* 2017). Australia is geographically located in the realm of both the Indian and Pacific Ocean and it has been demonstrated that the Australian climate is influenced by ENSO and IOD in different regions and seasons (McBride & Nicholls 1983; Power *et al.* 1999; Saji *et al.* 1999; Wang & Hendon 2007; Cai *et al.* 2009; Kiem & Verdon-Kidd 2010; Chowdhury & Beecham 2010, 2013; Gallant *et al.* 2012). ENSO is associated with rainfall over much of the continent, predominantly in the north and east, and the regions of influence shift with different seasons. IOD is especially important in the June–October period, which affects much of the wet season in the southwest and southeast (Risbey *et al.* 2009; Ummenhofer *et al.* 2009; Pepler *et al.* 2014).

ENSO and IOD affect Australian rainfall through extra-tropical and tropical teleconnections prompted by tropical sea surface temperature (SST) variations. According to Cai *et al.* (2011) Southern Oscillation (SO) is the main direct tropical teleconnection during ENSO and its impact on

doi: 10.2166/wcc.2018.146

Australian rainfall is confined to near-tropical parts of eastern Australia. During El Niño rainfall is blocked as near-tropical eastern Australia directly experiences subsidence and higher surface pressure which is associated with the western pole of the SO, while the impacts on extratropical Australian rainfall are proposed to stem mainly from the Rossby wave trains forced by convective variations in the Indian Ocean, for which the IOD is a main source of variability. These equivalent-barotropic Rossby wave trains originating from the Indian Ocean trigger changes to the midlatitude westerlies across southern Australia, therefore affecting rainfall through changes in mean state baroclinicity, west–east steering and possibly orographic effects (Cai *et al.* 2011).

The cool (positive) phase of ENSO, which is associated with cooler than average SSTs in the central and eastern tropical Pacific Ocean, is known as La Niña. La Niña events generally result in above-average rainfall over much of Australia (Verdon *et al.* 2004). In contrast, the warm (negative) phase of ENSO is associated with warmer than average SSTs in the central and eastern tropical Pacific Ocean. This phase of ENSO is known as El Niño, the occurrence of which generally results in below-average rainfall over much of eastern Australia (Wang & Hendon 2007). A neutral phase also exists, which is neither El Niño nor La Niña conditions.

The positive IOD (pIOD) is related to cooler than normal water in the tropical eastern Indian Ocean and warmer than normal water in the tropical western Indian Ocean (Saji *et al.* 1999). pIOD conditions are linked with decreased rainfall over the southern and central parts of Australia. On the other hand, a negative IOD (nIOD) results in warmer than normal water in the tropical eastern Indian Ocean and cooler than normal water in the tropical western Indian Ocean. nIOD events are linked to increased rainfall over parts of southern Australia (Gallant *et al.* 2012). The neutral IOD is the normal condition, where neither pIOD nor nIOD occurs. It is established that ENSO and IOD affect cool season rainfall in Australia (Cai *et al.* 2011). Meyers *et al.* (2007) proposed a method to identify the negative or positive phase of ENSO and IOD and applied the method to classify the years of 1876 to 1999 into the different phases. Later, Ummenhofer *et al.* (2009) extended the classification to more recent years.

Southeast Australia has experienced several severe droughts including the Federation Drought (1895–1902), the World War II drought (1937–1945) and the 'Big Dry' (post-1995). There has been considerable research in recent years with regard to the interactions of the ENSO and IOD and their influence on southeast Australian rainfall (e.g., Meyers *et al.* 2007; Cai *et al.* 2009, 2012; Kiem & Verdon-Kidd 2009; Risbey *et al.* 2009; Ummenhofer *et al.* 2009; Verdon-Kidd & Kiem 2009). However, there is a difference of opinion on the most effective phases of ENSO and IOD on seasonal rainfall in Australia. Ummenhofer *et al.* (2009) indicate that the 20th century big droughts in southeast Australia were driven by Indian Ocean variability and not the Pacific Ocean conditions for the June–October period. Moreover, it is discussed that lack of nIOD events is observed throughout the droughts of the 20th century. On the other hand, Cai *et al.* (2009, 2012) relate the rainfall reduction to an increase in pIOD events during winter and spring. This study is motivated by the need to better understand how ENSO and IOD affect Victoria's cool seasonal rainfall. At first thought, this seems to be a solved problem as extensive research has been carried out in order to understand the effect of climate modes on Australia, and particularly southeast Australia where Victoria is located (Verdon & Franks 2005; Cai *et al.* 2009, 2011; Ummenhofer *et al.* 2009). However, unlike other parts of Australia, such as NSW and Queensland, Victoria does not show strong correlation with the climate modes under study (Verdon-Kidd & Kiem 2009).

Moreover, the majority of the studies in the realm of understanding the influence of ENSO and IOD on cool seasonal rainfall across Australia are focused on June–October average rainfall (Risbey *et al.* 2009; Ummenhofer *et al.* 2009; Hudson *et al.* 2011). While the results of such studies show reduction (increase) of average rainfall for the period of study (i.e., June–October) during dry (wet) phases of ENSO and IOD, it is not well established which part of this period, i.e., June–August (austral winter) or September–November (austral spring), is carrying a higher weight regarding rainfall variation, particularly in Victoria. This study focuses on investigating first whether the state of Victoria has similar rainfall drivers as the rest of broader southeast Australia; and second what is the temporal pattern of the influence of the drivers across June–August rainfall average (austral winter) and September–November rainfall average (austral spring), as opposed to June–October rainfall average. Linear regression analysis is used to gain for the general understanding of the influence of the drivers on Victoria's seasonal rainfall, while classification analysis is used to investigate the effective phases of each climate mode during austral winter and spring.

STUDY AREA AND DATA

In this study, three distinct regions, i.e., east, central and west Victoria, are considered as case studies. Nine stations with the most complete records of data were selected from the chosen regions. Figure 1 shows the location details of the stations considered in this study. Monthly records of rainfall for 110 years (1900–2009) were obtained from the Bureau of Meteorology (BoM) for this study. Winter (June–August) and spring (September–November) rainfall were obtained from the monthly rainfall data. Table 1 shows the geographical locations of the stations, their annual mean rainfall and the percentage of monthly missing values for each station.

In order to investigate the SST and SLP anomalies, the monthly Niño3.4 and Southern Oscillation Index (SOI)

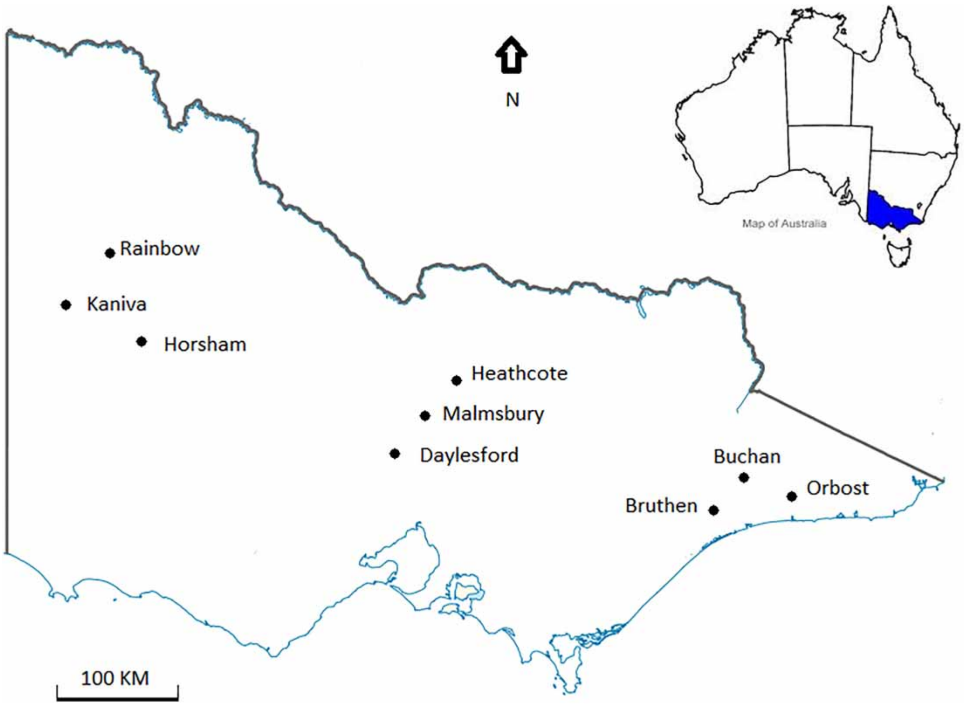

Figure 1 | Schematic map of the study area.

Table 1 | Details of geographical location and recorded data of rainfall stations of the study

Region	Site No.	Site name	Latitude	Longitude	Annual mean rainfall (mm)	% of missing observations
East	084003	Bruthen	37.71° S	147.83° E	759.5	0
	084005	Buchan	37.50° S	148.17° E	824.2	0
	084030	Orbost	37.69° S	148.46° E	845.1	0
Center	088042	Malmsbury	37.2° S	144.37° E	726.0	0
	088020	Daylesford	37.34° S	144.16° E	879.3	1
	088029	Heathcote	36.96° S	144.69° E	575.9	1
West	079023	Horsham	36.66° S	142.07° E	447.3	0
	078078	Kaniva	36.37° S	141.24° E	452.1	1
	077051	Rainbow	35.94° S	141.94° E	349.0	2

are used to construct the seasonal ENSO indicators and the monthly Dipole Mode Index (DMI) is used for construction of the seasonal IOD indicator. Monthly values of Niño3.4, SOI and DMI were obtained from Royal Netherlands Meteorological Institute (KNMI) Climate Explorer website (http://climexp.knmi.nl/). Table 2 summarizes the climate indices used in this study. Figures 2 and 3 show the intensity of the climate modes during the period of study.

LINEAR ANALYSIS

According to Cai *et al.* (2011), ENSO is largely unrelated to the IOD during austral winter and therefore its impact on southern latitude rainfalls in Australia is limited in winter.

Table 2 | Climate indices investigated as potential predictors of Victoria's seasonal rainfall

Predictors	Predictor definition	Region	Data source
SOI	Anomaly of mean sea level pressure (MSLP) difference between Tahiti and Darwin	Pacific	KNMI Climate Explorer
Nino3.4	Average SST anomaly over 5° S–5° N and 170°–120° W	Pacific	KNMI Climate Explorer
DMI	West Pole Index–East Pole Index: (Average SST anomaly over 10° S–10° N, 50°–70° E) – (Average SST anomaly over 10°S–Equator, 90°–110° E)	Indian	KNMI Climate Explorer

While most of the southeast Australian rainfall studies are focused on the June–October period, this study divides the Australian cool season into austral winter (June–August) and austral spring (September–November). In order to better visualize the seasonal temporal variation of rainfall during austral spring and winter, the rainfall data were smoothed using three-year running mean (Figure 4). The mean and standard deviation of the three-year seasonal running mean is shown in Table 3 for the two seasons under study. It can be seen that the June–October rainfall is highly variable during winter and spring. In east Victoria spring rainfall is higher than winter rainfall with an average of 72.8 mm compared to an average of 64.5 mm; however, winter rainfalls are higher than spring in central and west Victoria. The difference of magnitude and pattern in winter and spring rainfall in the region highlights the necessity of analysing the June–October rainfalls based on two separate seasons. The high variability of rainfall during different years makes the analysis of the effect of climate modes on rainfall in this region challenging; therefore, in order to develop reliable forecast models, the effect of the climate modes on the cool season rainfalls are in need of more investigation.

ENSO and IOD have a strong interaction, La Niña events tend to occur with nIOD events and El Niño years coincide with pIOD events. IOD is strongly correlated with ENSO in austral spring and it is less correlated with ENSO in winter; however, the independent and dependent impacts of IOD and ENSO are felt in both seasons in

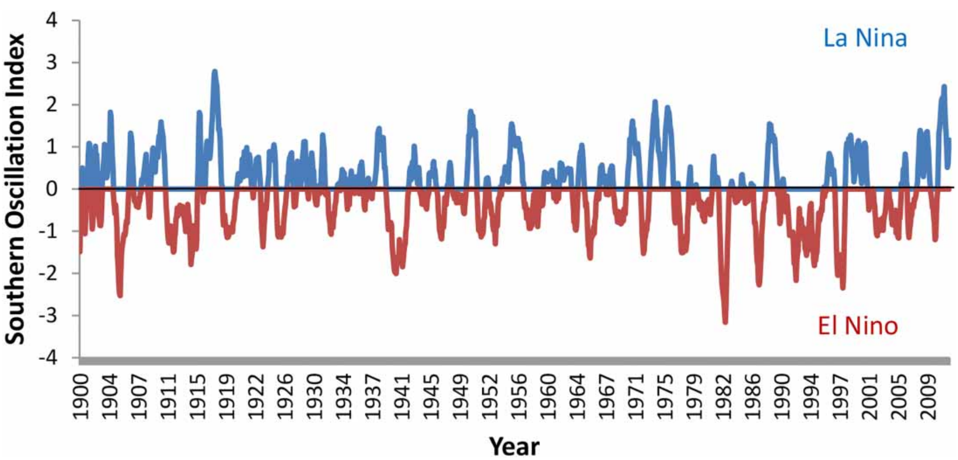

Figure 2 | SOI five-month running mean for the period 1900–2009 (*Data source:* http://climexp.knmi.nl/).

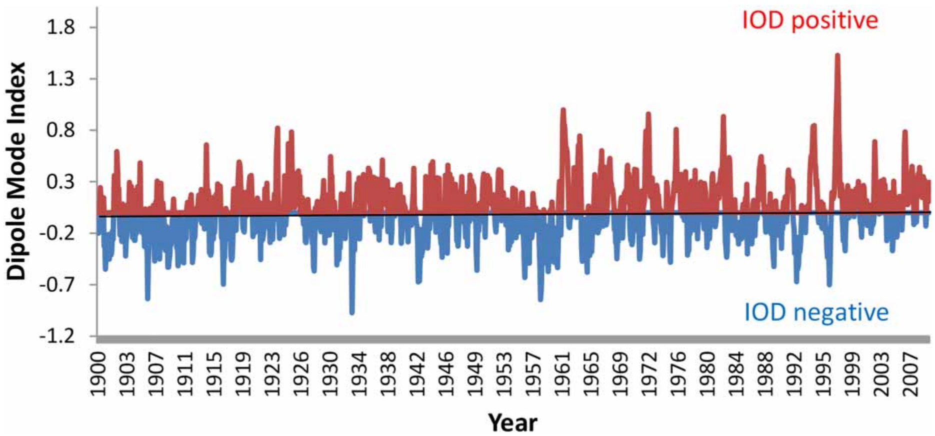

Figure 3 | IOD monthly values for the period 1900–2009 (*Data source:* http://climexp.knmi.nl/).

Australia (Cai *et al.* 2011). The dependent and independent effect of IOD and ENSO in Victoria in particular is investigated in this section. In order to show the strength of the relationship between IOD and ENSO in different seasons, Pearson correlations analysis between Niño3.4, SOI (ENSO indicators) and DMI (IOD indicator) is carried out for the four seasons (Figure 5). Figure 5 shows that there is a moderate to weak relationship between IOD and ENSO in spring and winter. Based on Figure 5, the relationship between ENSO and IOD in spring is stronger than in winter, with maximum correlation coefficient of 0.59 compared to -0.40 for winter.

In order to evaluate the linear relationships between spring and winter rainfall in Victoria with ENSO and IOD, linear regression analysis and partial regression analysis are conducted for the three regions under study. Partial regression is applied to investigate the independent effect of ENSO and IOD on seasonal rainfall, which involves the computation of the linear dependence of ENSO (IOD) upon seasonal rainfall after the linear relationship with IOD (ENSO) is removed from both ENSO (IOD) and seasonal rainfall. As the predictors are SOI, Niño3.4 and IOD, the analysis is carried out by removing the effect of IOD from SOI ($SOI_{(DMI)}$), IOD from Niño3.4 ($Nino3.4_{(DMI)}$), SOI from IOD ($DMI_{(SOI)}$) and Nino3.4 from IOD ($DMI_{(Ni3.4)}$). The results show that when the influence of IOD is removed from ENSO, SSTs anomalies in the Pacific Ocean (Niño3.4 indicator) have no effect on spring rainfall across Victoria and affect winter rainfall mildly in west Victoria (Tables 4 and 5). Furthermore, by removing the inter-correlations between ENSO and IOD, SSTs anomalies in the Indian Ocean (IOD) and SLPs anomalies in the Pacific Ocean (SOI) have weak relationships with austral spring and winter rainfall in central and west Victoria and no effect on east Victoria. The results propose that the climate modes affect east Victoria's spring rainfall mildly and only when ENSO and IOD occur simultaneously, reinforcing the effect of each other. Although by shifting towards central and west Victoria, the effect of climate modes on spring rainfall increases, the partial correlations show the independent effect of ENSO and IOD on these regions can be considered moderate to weak. The results are further verified in the section below.

CLASSIFICATION ANALYSIS

The regression analysis to some extent exhibits the strength of the influence of the climate modes on seasonal (spring and winter) rainfalls in Victoria. In order to verify the results of the linear analysis and determine which of the phases of ENSO (i.e., El Niño – La Niña) and IOD (i.e., pIOD – nIOD) contribute most to this effect, classification analysis is performed. Seasonal rainfall anomalies are calculated for the three regions of the case study (east, centre and west Victoria) based on Equation (1):

$$x_{i(anom)} = x_i - \bar{x} \tag{1}$$

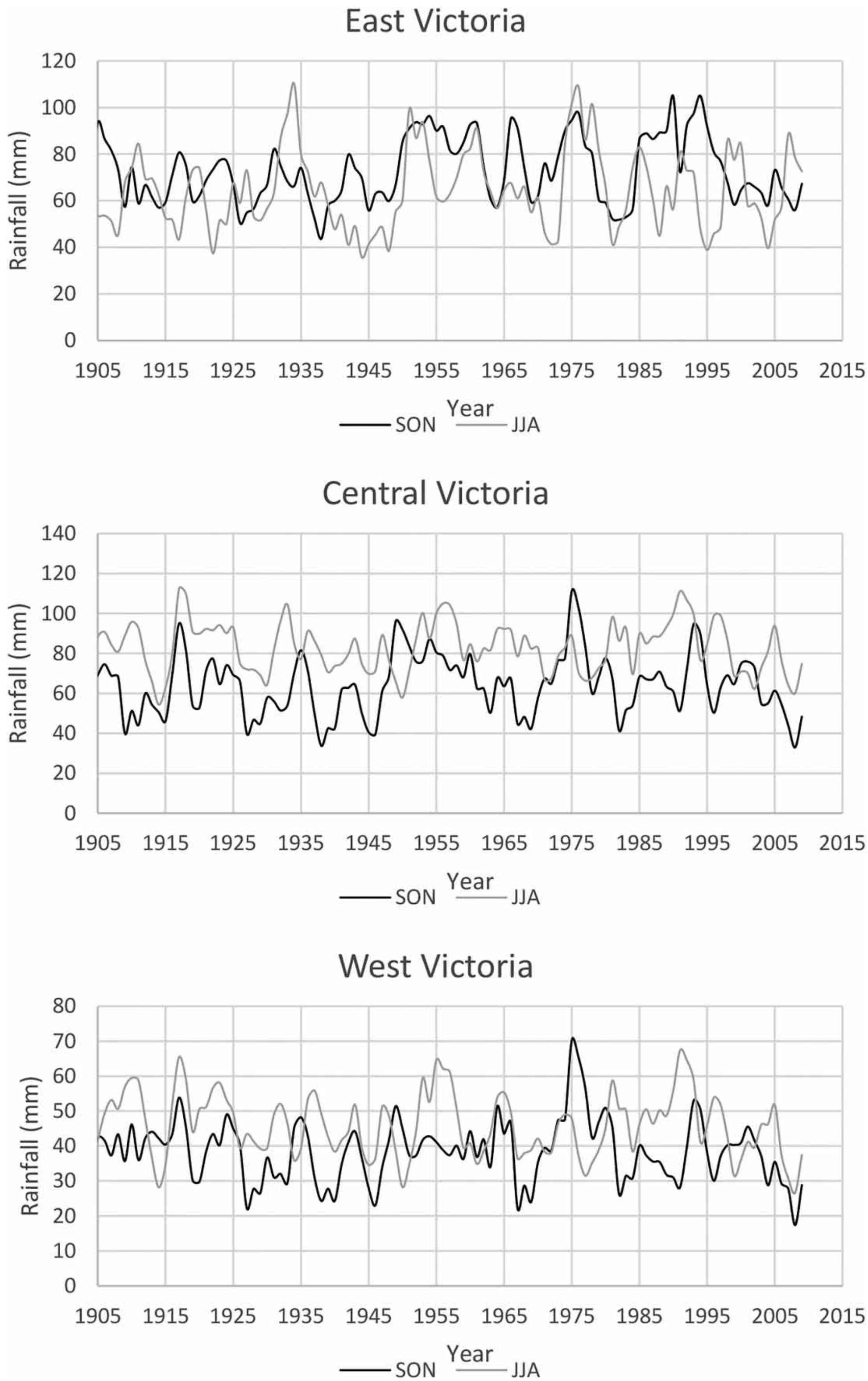

Figure 4 | Temporal cool season variation of rainfall (three-year running average) in East, Central and West Victoria for June–August (JJA) and September–November (SON).

Table 3 | Mean and standard deviation of three-years running mean seasonal rainfall for Victoria (1900–2009)

	Winter		Spring	
Region	Mean	STD	Mean	STD
East	64.5	16.8	72.8	14.00
Central	82.7	12.6	63.8	15.2
West	45.7	9.1	38.3	8.8

where $x_{i(anom)}$ is the anomaly of seasonal rainfall at year i, x_i is the value of seasonal rainfall at year i, and $\bar{x}$ is the long-term average rainfall for the particular season under study. The long-term average is calculated for the years 1900–2009 and the anomalies are created for this period.

Using Ummenhofer *et al.* (2009) classifications of ENSO and IOD years (Table 6), spring and winter rainfall anomalies are categorized based on the phases of ENSO and IOD (neutral ENSO, El Niño and La Niña; neutral IOD, pIOD and nIOD) and their co-occurrence. It is expected that the rainfall anomalies during the neutral phase of climate are normal rainfall with statistically significant zero median. A statistically significant zero median is referred to as normal climate condition and normal rainfall. The aim of the classification is to evaluate whether during different phases of climate, rainfall anomalies differ from normal rainfall (neutral condition); therefore, it is expected that the median of each group is statistically different from zero. Classifying ENSO and IOD results in nine different states of climate, of which, two seldom occur. The seven common states are El Niño–pIOD, pure El Niño, pure pIOD, neutral, pure La Niña, La Niña–nIOD and pure nIOD. The term 'pure' is used in the present study to identify that the only active phase of climate is the phase where the term 'pure' is used and the other mode is in neutral state. To investigate the reinforcement effect of ENSO and IOD on rainfall, this

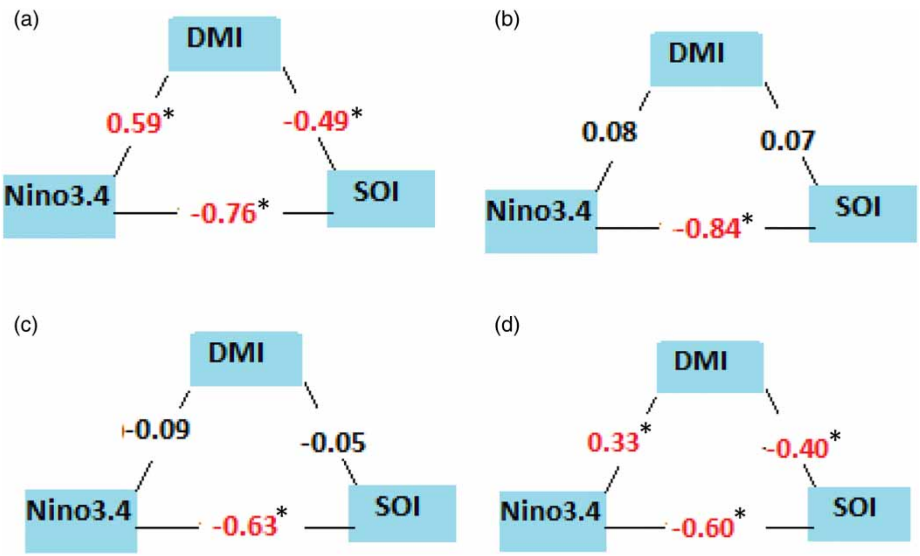

Figure 5 | Pearson correlation coefficients (r) of climate indices: (a) spring, (b) summer, (c) fall and (d) winter. Significant correlations are highlighted with an asterisk.

Table 4 | Regression and partial regression of ENSO and IOD indicators with spring rainfall (p value <0.05)

	SOI	$SOI_{(DMI)}$	Niño3.4	$Niño3.4_{(DMI)}$	DMI	$DMI_{(SOI)}$	$DMI_{(Ni3.4)}$
East	0.21	–	−0.27	–	−0.25	–	–
Center	0.43	0.27	−0.38	–	−0.44	−0.29	−0.29
West	0.43	0.27	−0.39	–	−0.45	−0.30	−0.29

Table 5 | Regression and partial regression of ENSO and IOD indicators with winter rainfall (p value <0.05)

	SOI	$SOI_{(DMI)}$	Niño3.4	$Niño3.4_{(DMI)}$	DMI	$DMI_{(SOI)}$	$DMI_{(Ni3.4)}$
East	–	–	–	–	–	–	–
Center	0.43	0.34	−0.21	–	−0.33	–	−0.28
West	0.33	0.24	−0.34	−0.27	−0.27	–	−0.19

Table 6 | The years of ENSO and IOD based on the Ummenhofer *et al.* (2009) classification

	Negative IOD	Neutral IOD	Positive IOD
El Niño	1930	1877, 1888, 1899, 1905, 1911, 1914, 1918, 1925, 1940, 1941, 1965, 1972, 1986, 1987	1896, 1902, 1957,1963, 1982, 1991, 1997, 2009
Neutral ENSO	1915, 1958, 1968, 1974, 1980, 1985, 1989, 1992	1880, 1881, 1882, 1883, 1884, 1895, 1898, 1900, 1901, 1904, 1907, 1908, 1912, 1920, 1921, 1927, 1929, 1931, 1932, 1934, 1936, 1937, 1939, 1943, 1947, 1948, 1951, 1952, 1953, 1953, 1959, 1960, 1962, 1966, 1967, 1969, 1971, 1976, 1977, 1979, 1983, 1990, 1993, 1995, 2001, 2002, 2003, 2005, 2006	1885, 1887, 1891, 1894, 1913, 1919, 1923, 1926, 1935, 1944, 1945, 1946, 1961, 1994, 2004, 2008
La Niña	1906, 1909, 1916, 1917, 1933, 1942, 1975	1878, 1879, 1886, 1889, 1890, 1892, 1893, 1897, 1903, 1910, 1922, 1924, 1928, 1938, 1949, 1950, 1954, 1955, 1956, 1964, 1970, 1973, 1978, 1981, 1984, 1988, 1996, 1998, 2000	1999, 2007

classification is used to categorize Victoria's spring and winter rainfall anomalies (Figures 6 and 7). The Wilcoxon signed rank test is applied to determine whether the median of each category of seasonal rainfall anomalies during different climate phases (i.e., El Niño–pIOD, pure El Niño, pure pIOD, pure La Niña, La Niña–nIOD and pure nIOD) is statistically significant from zero (Tables 7 and 8). For Figures 6 and 7 the neutral years are in the middle of each figure, with the dry phases (i.e., El Niño–pIOD, El Niño, pIOD) on the left and wet phases (i.e., La Niña–nIOD, La Niña, nIOD) on the right. The middle line in each bar shows the median rainfall.

In east Victoria, La Niña, nIOD, and their co-occurrence have no effect on spring rainfall meaning that the wet phases of ENSO and IOD do not affect east Victoria. Out of all the years of pIOD and El Niño, only in the years where El Niño and pIOD occur together is east Victoria's spring rainfall affected, i.e., years 1902, 1957, 1963, 1982, 1991, 1997, 2009. The median rainfall anomaly of −20 mm is recorded for east Victoria during the co-occurrence of El Niño–pIOD with all but one event out of seven showing below average rainfall.

In central Victoria during the wet phases of ENSO and IOD, only pure La Niña years show significant increase in spring rainfall, i.e., years 1903, 1910, 1922, 1924, 1928, 1938, 1949, 1950, 1954, 1955, 1956, 1964, 1970, 1973, 1978, 1981, 1984, 1988, 1996, 1998, 2000. A median of +12 mm during pure La Niña years is recorded with 16 out of 21 events having above average rainfalls. The effect of the dry phases (El Niño and pIOD) of ENSO and IOD on spring rainfall in central Victoria is only statistically significant during the pure years of each phase, i.e., for El Niño the years 1905, 1911, 1914, 1918, 1925, 1940, 1941, 1965, 1972, 1986, 1987 and for pIOD the years 1913, 1919, 1923, 1926, 1935, 1944, 1945, 1946, 1961, 1994, 2004, 2008. For central Victoria, a median rainfall anomaly of −22 mm is recorded during pure El Niño events with all but two events out of eleven having below average rainfall. Furthermore, a median of −20 mm is recorded for central Victoria during pure pIOD events with all but one event out of twelve showing below average rainfall.

West Victoria is the only region where the influence of La Niña–nIOD co-occurrence is felt with six events out of seven having above average rainfall in spring with a median of

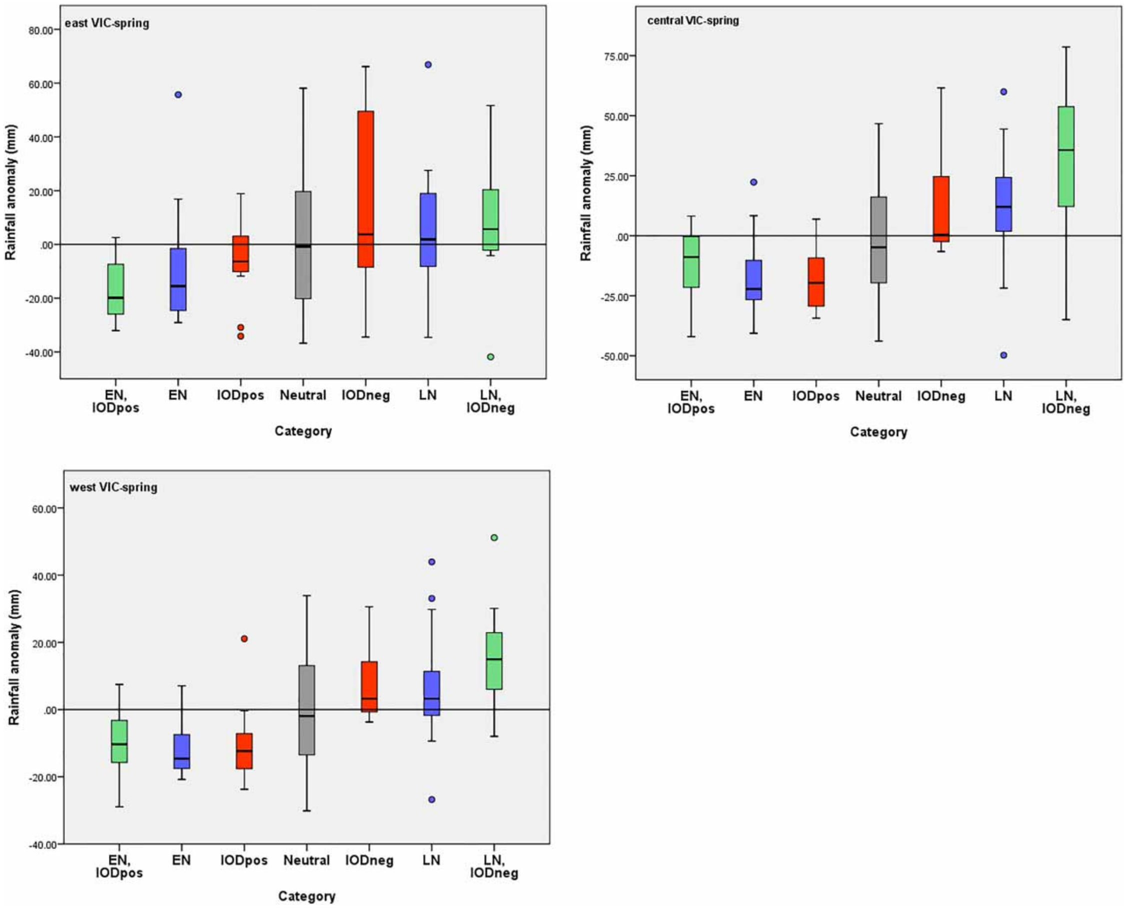

Figure 6 | Spring rainfall anomalies for the ENSO and IOD phases in Victoria. The neutral years are in the middle of each panel with El Niño–pIOD, El Niño and pIOD on the left and La Niña–nIOD, La Niña and nIOD on the right. The middle line in each bar shows the median rainfall.

+15 mm. The dry phases affect this region only when they are in their pure phases, i.e., for El Niño the years 1905, 1911, 1914, 1918, 1925, 1940, 1941, 1965, 1972, 1986, 1987 and for pIOD the years 1913, 1919, 1923, 1926, 1935, 1944, 1945, 1946, 1961, 1994, 2004, 2008. For west Victoria, a median rainfall anomaly of −15 mm is recorded during pure El Niño events with all but two events out of eleven having below average rainfall. A median of −12 mm is recorded for west Victoria during pure pIOD events with all but one event out of twelve showing below average rainfall.

By separating the influence of ENSO and IOD during winter it was found that none of the ENSO and IOD phases affect Victoria except for central Victoria where La Niña–nIOD co-occurrence affects the winter rainfall (Table 8).

The results show that there is an asymmetry in the effect of different phases of ENSO and IOD on Victoria's cool season (spring and winter) rainfall, i.e., both impact and temporal asymmetry can be seen. For better understanding of the mechanism responsible for the impact and temporal asymmetry seen in the results of the classification analysis, the development time frame and strength of IOD and ENSO for strongest ENSO and IOD years are investigated. For this purpose, the years with DMI values greater than one standard deviation (σ) (Lim & Hendon 2017) for five consecutive months are selected as strong pIOD events and the years with absolute DMI values greater than half standard deviation (0.5σ) are selected as strong nIOD events. The analysis of the DMI values showed that absolute DMI values in years classified as nIOD events (Table 6) are generally lower compared to pIOD events and finding five

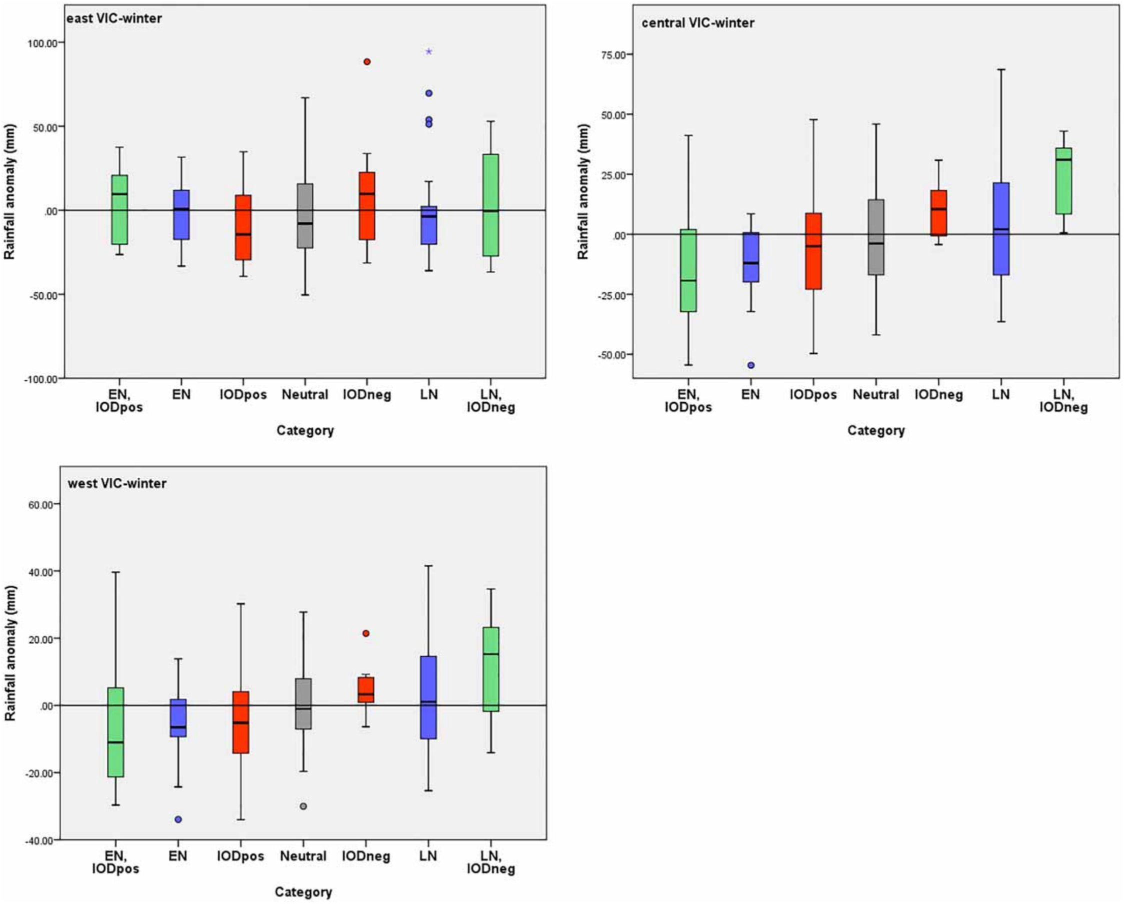

Figure 7 | Winter rainfall anomalies for the different ENSO/IOD categories in Victoria. The neutral years of ENSO and IOD are in the middle of each panel with El Niño and pIOD on the left and La Niña and nIOD on the right. The middle line in each bar shows the median rainfall.

consecutive months absolute DMI value greater than one standard deviation is not practical, therefore half standard deviation is proposed as the criteria for strong nIOD events. Among the years classified as strong pIOD events using the described method, the years 1961, 1994, 1997 and 1982 are chosen as the former two are pure pIOD and the two latter are pIOD–El Niño events. These years are consistent with Cai *et al.* (2014), who reported 1961, 1994 and 1997 as extreme pIOD events. Among strong nIOD events, the years 1916, 1933, 1958 and 1974 are selected as the latter two are pure nIOD and the former two are nIOD–La Niña events.

A similar approach is conducted to find strong El Niño and La Niña events based on NOAA's Oceanic Niño Index (ONI), which is the three-month running average SST anomaly for the Niño3.4 region (NOAA). NOAA considers

Table 7 | Wilcoxon signed rank test for spring rainfall

Region	EN,IOD +	EN	IOD +	Neutral	IOD −	LN	LN,IOD −
East	0.028[a]	–	–	–	–	–	–
Centre	–	0.026[a]	0.005[a]	–	–	0.035[a]	–
West	–	0.013[a]	0.028[a]	–	–	–	0.043[a]

[a]The significance level is 0.05.

Table 8 | Wilcoxon signed rank test for winter rainfall

Region	EN,IOD+	EN	IOD+	Neutral	IOD−	LN	LN,IOD−
East	–	–	–	–	–	–	–
Centre	–	–	–	–	–	–	0.018[a]
West	–	–	–	–	–	–	–

[a]The significance level is 0.05.

dry and wet episodes based on a threshold of ±0.5 °C for a minimum of five consecutive over-lapping seasons. After constructing the ONI values, the years where ONI is greater than nearly three times the threshold ($1.4 < |ONI|$) for five consecutive overlapping seasons are considered as strong El Niño/La Niña events (Finkl & Makowski 2017). The years 1877, 1987 (pure El Niño), 1942, 1988 (pure La Niña), 1902, 1997 (El Niño–pIOD) and 1955, 1975 (La Niña–nIOD) are selected as strong ENSO events. DMI and ONI in the selected strong IOD and ENSO years are plotted in Figures 8 and 9, respectively.

It is already established that IOD typically matures in austral spring while ENSO is well developed by austral winter and spring (Cai *et al.* 2011). Examining the extreme episodes of ENSO and IOD clearly shows that even during extreme events, as seen in Figures 8 and 9, ENSO and IOD are still much weaker in winter compared to spring. On the other hand, as discussed earlier, episodes of nIOD events show weaker DMI values compared to episodes of pIOD events (Figure 8) and La Niña events have lower ONI values compared to El Niño events (Figure 9). Therefore, the authors propose that the time frame development of ENSO and IOD, the difference in the strength of the dry phases compared to the wet phases together with the higher frequency of occurrence of the dry phases results in stronger effect of the dry phases of ENSO and IOD on austral spring rainfall compared to austral winter rainfall in this region, as discussed in the classification analysis. Cai *et al.* (2009, 2012) also relates the rainfall reduction in the cool season in Australia to an increase in pIOD events. Cai *et al.* (2011) also indicates that prediction of Australian climate not only depends on the skill to predict the phases and occurrence of ENSO, but also on the skill to predict related SST/convective variations in the eastern Indian Ocean (EIO), which are the main source of the Rossby wave trains that cause rainfall variations across the southern parts of the country. The impact of ENSO on southeast Australia during austral spring is conducted via the tropical Indian Ocean (TIO). Cai *et al.* (2012) showed that a strong asymmetry exists among the positive and negative phases

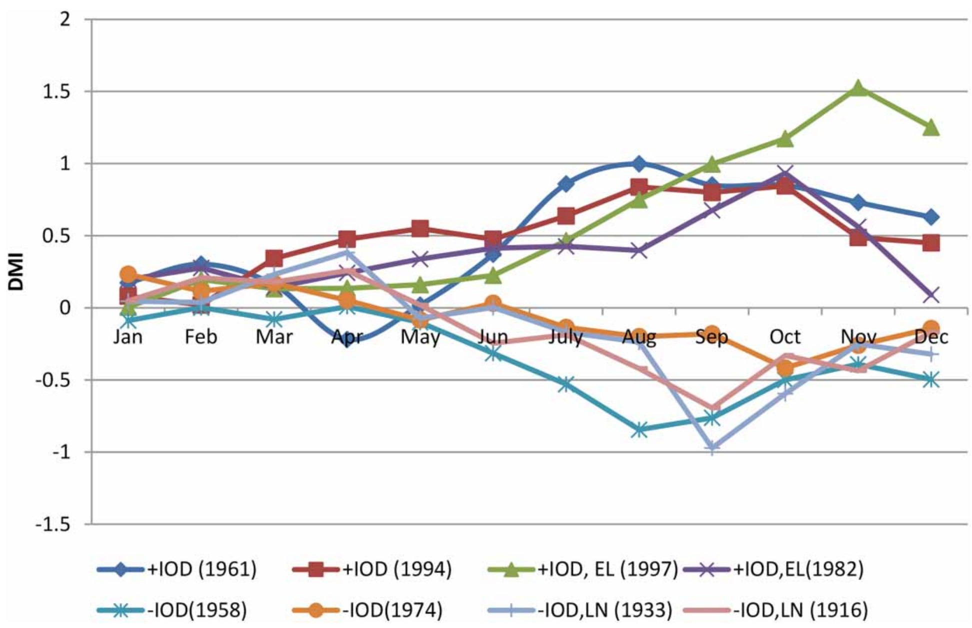

Figure 8 | DMI values for strong pIOD/nIOD events.

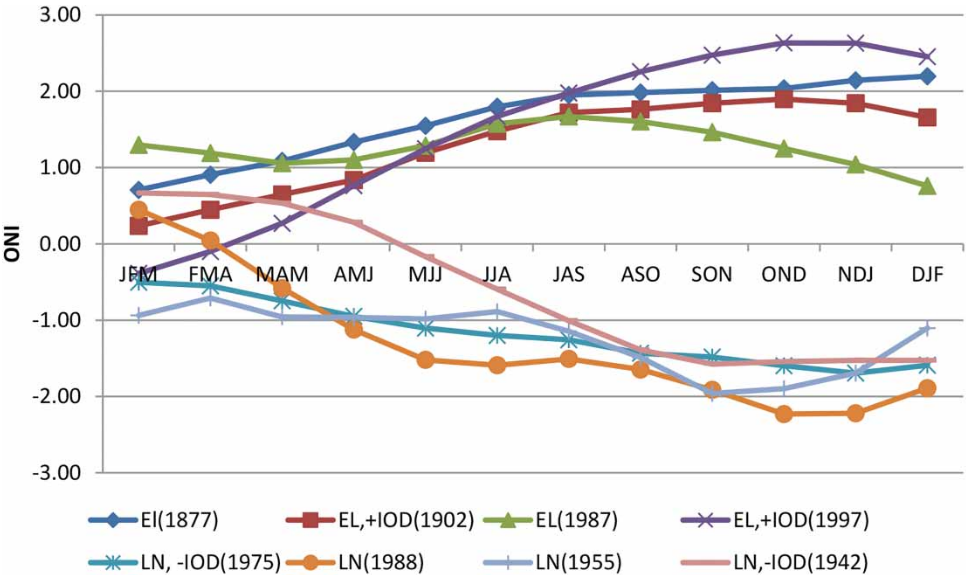

Figure 9 | ONI for strong El Niño/La Niña years.

of ENSO and IOD. For ENSO, only the impact of El Niño is carried out through the TIO pathway, while for La Niña the impact is delivered through the Pacific–South America pattern. For IOD, a greater convection anomaly and wave train response happens during pIOD events than during nIOD events. Furthermore, Cai *et al.* (2012) indicate that the coherence between the pIOD and El Niño is much higher compared to nIOD and La Niña, which suggests that the extratropical impact of El Niño via TIO is probably greater and more systematic than that of La Niña. The authors suggest that the mechanism discussed by Cai *et al.* (2012) may be the cause of the temporal and impact asymmetry seen in the effect of ENSO and IOD on Victoria's cool season rainfall. However, taking into account the discussed teleconnection and asymmetry among ENSO and IOD, the authors propose further research in this domain is required to fully understand the detailed mechanism of the tropical and extratropical teleconnections driving Victoria's rainfall during austral winter and spring.

CONCLUSION

With the aim of achieving better correlations and forecasting regime, this study investigated the effect of different phases of ENSO and IOD on seasonal rainfall in Victoria, Australia. The study takes into account the two approaches of linear analysis and classification analysis. The linear analysis, to some extent, revealed the strength of the effect of ENSO and IOD on cool seasonal rainfall in Victoria, bringing to attention the extent of the effect on spring compared to winter rainfalls.

The influence of ENSO and IOD is separated through partial regression and classification analysis. In east Victoria, La Niña, nIOD and their co-occurrence have no significant effect on spring rainfall, i.e., the wet phases of ENSO and IOD do not affect east Victoria. Out of all the years of IOD and El Niño, only the years where El Niño and pIOD occur together affect east Victoria's rainfall. In central Victoria, out of all the years of La Niña only pure La Niña years affect spring rainfall. The effect of the dry phases of ENSO and IOD (i.e., El Niño and pIOD) on spring rainfall in central Victoria is only during the pure years of each phase. In west Victoria, the effect of La Niña and nIOD is significant in spring only when they occur together. West Victoria is the only region where the influence of La Niña–nIOD co-occurrence is felt. The dry phases affect this region only when they are in their pure phases. In summary, rainfall anomalies during pure nIOD events, pure La Niña events and when they both occur at the same time (i.e., wet phases) are mostly variable; however, pure El Niño years, pure pIOD events and the co-occurrence of El Niño–pIOD (i.e., dry phases) consistently result in dry conditions during spring in Victoria. Furthermore, it was found that, contrary to the general notion regarding southeast Australia's rainfall, winter rainfall is less affected by the phases of climate modes compared to spring rainfall in Victoria.

REFERENCES

Barsugli, J. J. & Sardeshmukh, P. D. 2002 Global atmospheric sensitivity to tropical SST anomalies throughout the Indo-Pacific basin. *Journal of Climate* **15** (23), 3427–3442.

Biabanaki, M., Eslamian, S. S., Koupai, J. A., Cañón, J., Boni, G. & Gheysari, M. 2014 A principal components/singular spectrum analysis approach to ENSO and PDO influences on rainfall in western Iran. *Hydrology Research* **45** (2), 250–262. doi:10.2166/nh.2013.166.

Cai, W., Cowan, T. & Sullivan, A. 2009 Recent unprecedented skewness towards positive Indian Ocean Dipole occurrences and its impact on Australian rainfall. *Geophysical Research Letters* **36** (11).

Cai, W., van Rensch, P., Cowan, T. & Hendon, H. H. 2011 Teleconnection pathways of ENSO and the IOD and the mechanisms for impacts on Australian rainfall. *Journal of Climate* **24** (15), 3910–3923.

Cai, W., Van Rensch, P., Cowan, T. & Hendon, H. H. 2012 An asymmetry in the IOD and ENSO teleconnection pathway and its impact on Australian climate. *Journal of Climate* **25** (18), 6318–6329.

Cai, W., Santoso, A., Wang, G., Weller, E., Wu, L., Ashok, K., Masumoto, Y. & Yamagata, T. 2014 Increased frequency of extreme Indian Ocean Dipole events due to greenhouse warming. *Nature* **510** (7504), 254–258.

Chattopadhyay, G., Chattopadhyay, S. & Jain, R. 2010 Multivariate forecast of winter monsoon rainfall in India using SST anomaly as a predictor: neurocomputing and statistical approaches. *Comptes Rendus Geoscience* **342** (10), 755–765.

Chowdhury, R. & Beecham, S. 2010 Australian rainfall trends and their relation to the southern oscillation index. *Hydrological Processes* **24** (4), 504–514.

Chowdhury, R. K. & Beecham, S. 2013 Influence of SOI, DMI and niño3. 4 on South Australian rainfall. *Stochastic Environmental Research and Risk Assessment* **27** (8), 1909–1920.

Finkl, C. W. & Makowski, C. 2017 *Coastal Wetlands: Alteration and Remediation*, Vol. 21. Springer, Cham, Switzerland.

Gallant, A., Kiem, A., Verdon-Kidd, D., Stone, R., Karoly, D. & de Michele, C. 2012 Understanding hydroclimate processes in the Murray-Darling Basin for natural resources management. *Hydrology and Earth System Sciences* **16** (7), 2049–2068.

Hajani, E. & Rahman, A. 2017 Characterising changes in rainfall: a case study for New South Wales State, Australia. *International Journal of Climatology*. http://onlinelibrary.wiley.com/doi/10.1002/joc.5258/epdf.

Hajani, E., Rahman, A. & Ishak, E. 2017 Trends in extreme rainfall in the state of New South Wales, Australia. *Hydrological Sciences Journal*. http://dx.doi.org/10.1080/02626667.2017.1368520.

Hartmann, H., Becker, S. & King, L. 2008 Predicting summer rainfall in the Yangtze River basin with neural networks. *International Journal of Climatology* **28** (7), 925–936.

Hudson, D., Alves, O., Hendon, H. H. & Marshall, A. G. 2011 Bridging the gap between weather and seasonal forecasting: intraseasonal forecasting for Australia. *Quarterly Journal of the Royal Meteorological Society* **137** (656), 673–689.

Ishak, E., Rahman, A., Westra, S., Sharma, A. & Kuczera, G. 2013 Evaluating the non-stationarity of Australian annual maximum floods. *Journal of Hydrology* **494**, 134–145.

Kiem, A. S. & Verdon-Kidd, D. C. 2009 Climatic drivers of Victorian streamflow: is ENSO the dominant influence. *Australian Journal of Water Resources* **13** (1), 17–29.

Kiem, A. & Verdon-Kidd, D. 2010 Towards understanding hydroclimatic change in Victoria, Australia – preliminary insights into the 'Big Dry'. *Hydrology and Earth System Sciences* **14** (3), 433–445.

Lau, K. & Weng, H. 2001 Coherent modes of global SST and summer rainfall over China: an assessment of the regional impacts of the 1997-98 El Niño. *Journal of Climate* **14** (6), 1294–1308.

Lim, E.-P. & Hendon, H. H. 2017 Causes and predictability of the negative Indian Ocean Dipole and its impact on La Niña during 2016. *Scientific Reports* **7** (1), 12619.

McBride, J. L. & Nicholls, N. 1983 Seasonal relationships between Australian rainfall and the Southern Oscillation. *Monthly Weather Review* **111** (10), 1998–2004.

Meyers, G., McIntosh, P., Pigot, L. & Pook, M. 2007 The years of El Niño, La Niña and interactions with the tropical Indian Ocean. *Journal of Climate* **20** (13), 2872–2880.

Pepler, A., Timbal, B., Rakich, C. & Coutts-Smith, A. 2014 Indian Ocean Dipole overrides ENSO's influence on cool season rainfall across the Eastern seaboard of Australia. *Journal of Climate* **27** (10), 3816–3826. Retrieved from http://www.scopus.com/inward/record.url?eid=2-s2.0-84900402016&partnerID=40&md5=61ea6e7c723d37cdca12fd90fb8157d7.

Power, S., Casey, T., Folland, C., Colman, A. & Mehta, V. 1999 Inter-decadal modulation of the impact of ENSO on Australia. *Climate Dynamics* **15** (5), 319–324.

Risbey, J. S., Pook, M. J., McIntosh, P. C., Wheeler, M. C. & Hendon, H. H. 2009 On the remote drivers of rainfall variability in Australia. *Monthly Weather Review* **137** (10), 3233–3253.

Saji, N. H., Goswami, B. N., Vinayachandran, P. N. & Yamagata, T. 1999 A dipole mode in the tropical Indian ocean. *Nature* **401** (6751), 360–363.

Shukla, R. P., Tripathi, K. C., Pandey, A. C. & Das, I. 2011 Prediction of Indian summer monsoon rainfall using Niño indices: a neural network approach. *Atmospheric Research* **102** (1), 99–109.

Ummenhofer, C. C., England, M. H., McIntosh, P. C., Meyers, G. A., Pook, M. J., Risbey, J. S. & Taschetto, A. S. 2009 What causes southeast Australia's worst droughts? *Geophysical Research Letters* **36** (4).

Verdon, D. C. & Franks, S. W. 2005 Indian Ocean sea surface temperature variability and winter rainfall: Eastern Australia. *Water Resources Research* **41** (9), 1–10.

Verdon, D. C., Wyatt, A. M., Kiem, A. S. & Franks, S. W. 2004 Multidecadal variability of rainfall and streamflow: Eastern Australia. *Water Resources Research* **40** (10), W10201.

Verdon-Kidd, D. C. & Kiem, A. S. 2009 On the relationship between large-scale climate modes and regional synoptic patterns that drive Victorian rainfall. *Hydrology and Earth System Sciences* **13** (4), 467–479.

Wang, G. & Hendon, H. H. 2007 Sensitivity of Australian rainfall to inter–El Niño variations. *Journal of Climate* **20** (16), 4211–4226.

Yufu, G., Yan, Z. & Jia, W. 2002 Numerical simulation of the relationships between the 1998 Yangtze River valley floods and SST anomalies. *Advances in Atmospheric Sciences* **19** (3), 391–404.

First received 30 August 2017; accepted in revised form 16 January 2018. Available online 22 February 2018